Coordinate Systems for Mapping Low-Altitude Trapped Particle Fluxes

DANIEL HEYNDERICKX AND JOSEPH LEMAIRE

Belgian Institute for Space Aeronomy, Brussels, Belgium

The widely used coordinate system (B, L) has proved very suitable for most of the region covered by the Van Allen belts, but is not very well suited for the low-altitude regions where the Earth's atmosphere interacts with the trapped particle population. Several alternative coordinate systems have been proposed that aim to take into account the steep flux gradients in the region of the upper atmosphere. An overview of these coordinates is presented. The effectiveness of each system is assessed by mapping the proton flux distribution of NASA's AP-8 model. Special attention is given to Hassitt's weighted average of the atmospheric density over the drift shells of trapped particles, which appears very efficient in mapping fluxes for low L values.

INTRODUCTION

Trapped particle fluxes usually are mapped in the (B, L) coordinate system [*McIlwain*, 1961]. While these coordinates have proved very suitable for most of the region covered by the Van Allen belts, they are not very well suited for the low-altitude regions where the Earth's atmosphere interacts with the trapped particle population. The concept of atmospheric cut-off is defined in the next section. An alternative coordinate has been proposed by Daly and Evans [1993] to take into account the steep flux gradients in the region of the upper atmosphere. This coordinate is discussed in the third section.

It is well known from previous studies that the cosmic ray intensity observed within the atmosphere depends on the quantity of absorbing material traversed before observation. Besides the magnetic rigidity effect, the barometric pressure has an appreciable effect on the measured cosmic ray intensity. This is why cosmic ray fluxes usually are reported in terms of atmospheric depth, i.e. the mass of air per unit area above the point of observation, or air pressure at the point of observation.

The same concept should also be applied to identify an equivalent atmospheric penetration depth of Van Allen belt particles. Evidence that the flux of Van Allen belt particles depends on the atmospheric density distribution has been forwarded by Pfitzer [1990], who found that the atmospheric density at space station altitudes is a better variable than B/B_0 to organise the AP-8 MIN and AP-8 MAX fluxes.

In order to estimate the influence of the Earth's atmosphere on the distribution of trapped particles, the effects of the atmosphere have to be averaged over the particle's orbit. Ray [1960] and Lenchek and Singer [1962] have derived expressions for the atmospheric density averaged over the orbit of a particle trapped in a dipole field. Newkirk and Walt [1964] have determined the average density for a realistic representation of the geomagnetic field. Hassitt [1965] has simplified considerably the procedure of Newkirk and Walt [1964], while maintaining the same accuracy. In the fourth section, we describe Hassitt's [1965] method and it's application to the study of low-altitude coordinate systems.

DEFINITION OF ATMOSPHERIC CUT-OFF

Trapped ions and electrons whose pitch angle is scattered in the loss cone, either by wave-particle interaction or Coulomb collisions with ions and electrons in the ionosphere, are dumped in the atmosphere where they lose their energy.

Some of these energetic particles are backscattered and re-enter the magnetosphere with a different energy. The penetration depth of the primaries into the atmosphere depends on their energy. Calculations of penetration depths have been given by Bailey [1959], Rees [1963] and Kamiyama [1966]. Electrons of 2 keV, vertically incident, penetrate down to 120 km altitude. When their energy is 1 MeV, they can penetrate down to 60 km altitude. Protons of 20 keV and 20 MeV penetrate down to 120 km and 60 km, respectively. Particles penetrating with a larger angle of incidence in the atmosphere dissipate their energy at higher altitudes.

The range of cut-off altitudes over which primary Van Allen belt particles are interacting most strongly with the neutral atmosphere is rather narrow (from 50 to 200 km) compared to the length of their drift path within the magnetosphere. Over this small altitude range the magnetic field intensity varies only slightly: an altitude variation corresponding to one atmospheric scale height of 50 km corresponds to a change of only a few percent in the value of B but of orders of magnitude in the energetic particle flux. This indicates how sensitive flux values provided by environment models are to even small inaccuracies and imprecisions in the value of B or B/B_0 (where B_0 is defined as $B_0 = 0.311653/L^3$) at low altitudes[1].

The locus of points of deepest penetration for trapped particles can be described by the magnetic cut-off field intensity $B_c(L)$. Among the family of drift shells (B, L), for a given L, B_c is the highest B value for which all particles on the drift shell (B, L) are trapped. Particles on drift

[1]Note that with the above definition, B_0 is an invariant of motion.

shells (B, L) with $B > B_c$ are precipitating or quasi-trapped particles. Since the separation between trapped and quasi-trapped particles is determined by the neutral atmosphere, B_c must be a function of the parameters influencing the density distribution of the atmosphere, such as A_p or K_p and mainly the solar radio flux $F_{10.7}$, which controls the heating of the upper atmosphere. In addition, B_c also depends on the particle energy E.

The thin atmospheric layer where the precipitated particles lose their energy can be considered as a rather abrupt absorbing wall. In the AP-8 [*Sawyer and Vette*, 1976] and AE-8 [*Vette*, 1991] trapped particle models, the omnidirectional integral flux $J(E, L, B/B_0)$ drops to zero for $B_c/B_0 = 0.6572\, L^{3.452}$, an empirical formula derived by Vette [1991] (note that with this definition B_c/B_0 also is an adiabatic invariant since it only depends on L). In the family of drift shells (B, L), the drift shell (B_c, L) is the one where the lowest altitude reached by a particle moving on this shell is 100 km. Whether the atmospheric cut-off is located at 100 km or 200 km altitude will not change significantly the equatorial loss cone angle $\alpha_{0c} = \arcsin\sqrt{B_0/B_c}$. Similarly, the equatorial pitch angle distribution $J(E, L, \alpha_0)$ will only depend significantly on B_c near $\alpha_0 = \alpha_{0c}$ and not at all near $\alpha_0 = 90°$.

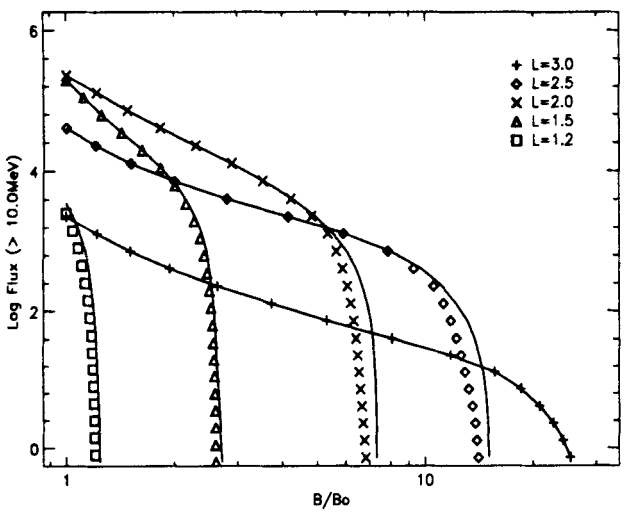

Fig. 1. The integral AP-8 MIN/MAX proton flux above 10 MeV as a function of B/B_0 for selected L-values. The symbols denote AP-8 MAX values, the AP-8 MIN values are represented by the solid lines.

Because of the very small variation of the magnetic field over the limited altitude range where the trapped particle flux decreases by several orders of magnitude, neither B, B/B_0, nor α_0 are appropriate coordinates to map omnidirectional or directional particle fluxes at low altitudes. Indeed, small inaccuracies in the determination of B or α_0 will result in large errors on the atmospheric cut-off altitude. To illustrate this point, we show in Fig. 1 the integral proton flux $J(> 10\,\text{MeV})$ in the AP-8 models [*Sawyer and Vette*, 1976]

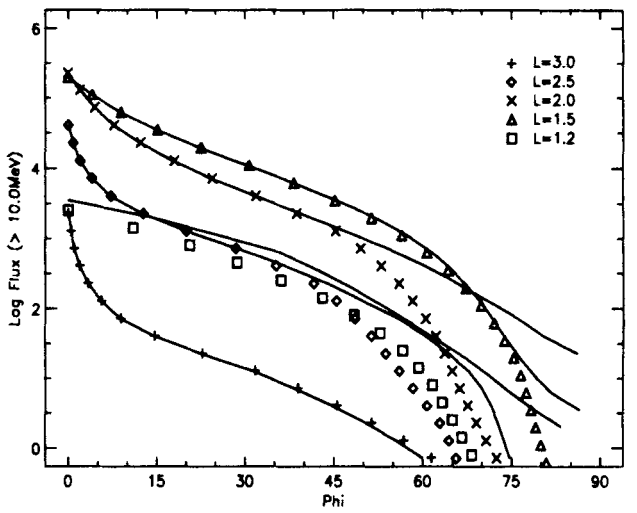

Fig. 2. The integral AP-8 MIN/MAX proton flux above 10 MeV as a function of φ for selected L-values. The symbols and lines have the same meaning as in Fig. 1.

as a function of B/B_0, for five values of L. The solid lines correspond to proton fluxes for minimum solar activity, the symbols to fluxes for solar maximum[2]. For L values below 3 the flux decreases almost vertically when B/B_0 approaches B_c/B_0. This steep gradient of J clearly makes an accurate determination of the particle flux by interpolation in B/B_0 difficult and coarse near the atmospheric cut-off. The dependence of the particle flux J on the equatorial pitch angle α_0 is equally steep near the loss cone angle α_{0c} and equally difficult to interpolate.

Alternative Coordinates

A useful alternative to B/B_0 has been proposed by Daly and Evans [1993]. While B/B_0 varies from a value close to 1 at the geomagnetic equator to a large value near the Earth's surface, the angle φ defined as

$$\varphi = \arcsin\left(\frac{B - B_0}{B_c - B_0}\right) \qquad (1)$$

varies from a value close to 0° at the equator to 90° at the atmospheric cut-off where $B = B_c$. The advantage of φ is that low-altitude variations in flux are spread over a larger range of variation of φ, so that interpolation between flux values becomes less difficult. This effect is illustrated in Fig. 2, which shows the dependence of the AP-8 MIN (solid line) and AP-8 MAX (symbols) fluxes on φ, for the same values of E and L as in Fig. 1.

However, it remains that the determination of the coordinate φ by means of Eq. (1) requires a magnetic field model with a very high accuracy and precision. In particular, near

[2]The vertical spacing of the points in Figs. 1, 2, 4 and 5 corresponds to a fixed decrement $\Delta \log J = 0.25$ in the block data of the NASA models. Instead of values for $\log J$, the corresponding increments $\Delta \log(B/B_0)$ are stored in the models.

the cut-off region the coordinate φ becomes very sensitive to the value chosen for B_c. It should be emphasized that the altitude corresponding to B_c depends on the energy of the particle and ranges between 50 and 200 km.

Daly and Evans [1993] used the following values for B_c/B_0:

$$\frac{B_c}{B_0} = \begin{cases} 0.66\,L^{3.452} & \text{for AP-8 MIN} \\ 0.65\,L^{3.452} & \text{for AP-8 MAX}, \end{cases} \quad (2)$$

which they obtained by fitting the maximum B/B_0 values in AP-8. Figure 3 shows the invariant altitude corresponding to the last value of B/B_0 of the L-blocks in the AP-8 models, for $E > 10$ MeV, as a function of L. The dotted and solid lines in this figure represent the invariant altitude for B_c as given by Eqs. (2). It can be seen that for $L \leq 2$ the invariant altitude corresponding to B_c for the solar minimum model lies above the minimum invariant altitudes of the model points, which means that the B_c values are too low. A better agreement is found by raising the coefficient in the fit function from 0.66 to 0.67 (we have used the coefficient 0.67 for Fig. 2). The corresponding invariant altitude is shown by the dashed line in Fig. 3. Below $L \simeq 2$ the field line segments in AP-8 terminate very close to or on the fitted B_c values. Above $L \simeq 2$ the proton flux in the models drops to zero before the cut-off region is reached.

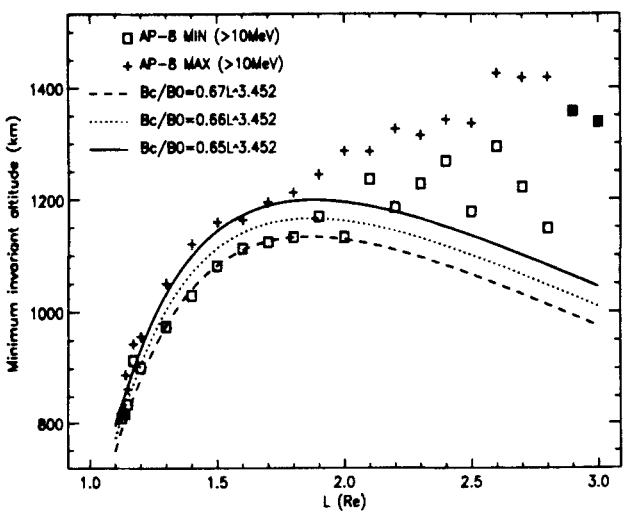

Fig. 3. Invariant altitudes corresponding to the last B/B_0 value of the L blocks in AP-8 MAX (+) and AP-8 MIN (□), for $E >$ 10 MeV. The lines show the invariant altitude corresponding to three fits of B_c/B_0.

Drift Shell Average of Atmospheric Density

Although the use of the coordinate φ makes the interpolation of low altitude fluxes more accurate, Def. (1) is a functional dependence chosen solely for its benefit of improving the numerical accuracy of the interpolation and has no physical grounds. Similarly, Def. (2) is an empirical relation that was found to fit the AP-8 model data.

It has already been pointed out by Pfitzer [1990] that the atmospheric density is a better coordinate to organise AP-8 proton fluxes at Space Station altitudes. He found that the AP-8 MIN and AP-8 MAX proton fluxes for Space Station altitudes (350–500 km) fall on almost the same curve when plotted as a function of the atmospheric densities for minimum and maximum solar activity conditions, respectively. Pfitzer's [1990] study confirms that at low altitudes the atmospheric density distribution governs the flux distribution of trapped protons. Note that the limited altitude range considered by Pfitzer corresponds to a restricted range of atmospheric density of 10^{-16}–10^{-14} g cm^{-3}. Our study covers the full range of atmospheric densities and altitudes.

The atmospheric density at a given altitude does not determine, however, the total mass of material traversed by a particle detected at that altitude. Instead, one should consider an average of the atmospheric density over an azimuthal drift path of particles of a given species and with a given energy.

Hassitt [1965] has developed a computer code at UCSD Physics Department which calculates the number density of atoms, ions, and molecules given by appropriate atmospheric and ionospheric models over a drift shell (B, L). A weighted average density $n_s(B, L)$ is then determined by multiplying the resulting number densities with the collision cross section σ_i of the trapped particles with the constituents i, summing over i and integrating the sum over the drift shell (B, L). C.E. McIlwain has kindly provided J. Lemaire with a revised version of Hassitt's original program, which we have modified further. In the following sections, we discuss the definition of $n_s(B, L)$ in more detail. A detailed description of the software package is given by Hassitt [1964] and by Heynderickx et al. [1994].

Definition of drift shell averaged density

Consider particles of energy E trapped on a drift shell (B, L). At a point P on the drift shell with geocentric coordinate vector $\vec{r}$, the number density $n_i(\vec{r})$ of atmospheric or ionospheric constituent i can be determined from suitable atmospheric and ionospheric models. We define a local weighted average density $n(\vec{r})$ as

$$n(\vec{r}) = \frac{\sum_i \sigma_i(E)\, n_i(\vec{r})}{\sigma_0}, \quad (3)$$

where $\sigma_0 = 10^{-15}\text{cm}^2$ is a normalization factor of the order of magnitude of the collision cross sections for trapped protons with atmospheric particles. The summation in Eq. (3) extends over all atmospheric, ionospheric and plasmaspheric constituents that interact with trapped particles. Note that originally Hassitt's [1964] code used constant values for the cross sections, while we implemented energy dependent cross sections.

The field aligned velocity component v_p of the trapped particles depends on their local pitch angle, being zero at the mirror points and reaching its maximum on the geomagnetic equator. Consequently, the particles spend more time in the

high density region around their mirror points than closer to the equator. To account for this effect when integrating the local average density n over the drift shell, we apply as a weight factor the time needed for the particles to move to a neighbouring point on the same field line during their bounce motion. The azimuthal drift velocity also is position dependent, so that a second weight factor, namely the time needed to drift to a neighbouring field line on the azimuthal drift motion, has to be used.

Let dx and dy denote elements of length along a field line and along the direction of azimuthal drift, respectively, and v_p and v_d the corresponding local drift velocities. A drift shell averaged atmospheric density n_s then can be defined as

$$n_s(B,L) = \frac{S(n,B,L)}{S(1,B,L)}, \tag{4}$$

with

$$S(n,B,L) = \iint n(\vec{r}) \frac{dx}{v_p} \frac{dy}{v_d}, \tag{5}$$

where the denominator in Eq. (4) serves as a normalisation factor and the integration in Eq. (5) extends over the whole drift shell.

Atmosphere and Ionosphere Models

We have updated Hassitt's code by including contemporary models for the neutral atmosphere, the ionosphere and the plasmasphere. A detailed description of the modified software can be found in Heynderickx et al. [1994].

The Mass-Spectrometer-Incoherent-Scatter (MSIS) neutral atmosphere model describes the neutral temperature and the densities of He, O, N_2, O_2, Ar, H, and N. The model version used in this study is MSISE-90 [*Hedin*, 1991].

The International Refererence Ionosphere (IRI) describes monthly averages of electron density, electron temperature, ion temperature, ion composition and ion drift in the altitude range from 50 km to 1000 km for magnetically quiet conditions in the non-auroral ionosphere. The IRI models are available at the National Space Science Data Center (NSSDC) [*Bilitza*, 1990]. D. Bilitza has kindly sent us the latest version, IRI-90.

Since the IRI-90 model is limited in altitude, an extension of the ion density into the magnetosphere is required to account for the small pitch angle scattering experienced by the trapped ions and electrons forming the radiation belts. It is usually held that pitch angle scattering of trapped particles is due to wave-particle interactions. In this study, we only consider the effects of collisions, since the wave spectrum distribution in the magnetosphere is less well known than the distribution of thermal ions and electrons.

Several three dimensional models have been proposed to describe the equatorial and field-aligned ionization density in the plasmasphere and plasmatrough. We have used the model of Carpenter and Anderson [1992] for the equatorial electron density. This model describes, in piecewise fashion, the "saturated plasmasphere", i.e. the region of steep plasmapause gradients, and the plasmatrough. The electron densities at non-equatorial latitudes above 1000 km were extrapolated along dipole field lines to fit the equatorial density distribution of Carpenter and Anderson [1992].

Collisional Cross Sections

The collisional cross section of trapped particles interacting with the neutral atmosphere and the ionosphere serves as a measure for the relative scattering efficiency of the various constituents and processes involved. The main processes to consider are: excitation and ionization of the target, dissociation for target molecules, charge exchange for protons on atoms and Coulomb interaction for charged particles. The relative importance of the different processes depends on the type of particles and the energy range. For each interaction, analytic expressions for the collision cross section as a function of the kinetic energy of the incident particle have been drawn from the literature and implemented in a computer program, CROSS [*Pierrard*, 1994]. CROSS takes as input the kinetic energy of the incident particle and the type of the incident and the target particles, and returns the total cross section for all relevant collision processes.

Results

We calculated the drift shell averaged density n_s for the AP-8 grid points represented in Fig. 1 with Hassitt's (1965) software, updated as described above. Figure 4 shows the dependence of these proton fluxes on n_s for $L = 1.2$ and $L = 1.5$. It can be seen that for both the solar maximum (MAX) and solar minimum (MIN) fluxes, the curves for the respective L values virtually coincide (this is also the case for intermediate values of L up to $L \simeq 1.7$, which are not shown in Fig. 4).

It thus seems that for low L-values the drift shell averaged density n_s is very well suited to represent the trapped particle distribution, as its eliminates the dependence of the flux on L.

The two curves for solar minimum in Fig. 4 diverge somewhat for the highest values of n_s. This may be due to inaccuracies in the AP-8 MIN model for very low altitudes. In Fig. 3, it can be seen that the lowest invariant altitude in AP-8 MIN displays some irregularity around $L = 1.2$ and especially for $L \geq 2.0$, where it fluctuates strongly.

Since we used extensive atmospheric and ionospheric models for the calculation of n_s, we expected the respective curves for solar minimum and maximum in Fig. 4 to be closer together, although they do overlap for the highest densities. Again, we need to re-investigate the solar minimum data, since AP-8 MIN resulted from the combination of different data sets.

For values of $L > 1.7$, the AP-8 flux vs. n_s curves, shown in Fig. 5, no longer coincide. From this we conclude that two different populations can be distinguished in the AP-8 models. Below $L \leq 1.7$ (the limiting value for L depends on the particle energy), the trapped particle flux is governed by the vertical distribution of the atmospheric density. At higher L values, the proton flux already reaches negligible values some distance above the atmospheric cut-off height. The value $L \simeq 1.7$ corresponds to the location of the maxi-

mum in the proton flux distribution for $E = 10\,\mathrm{MeV}$. This explains the lowering of the curves in Fig. 5 corresponding to progressively higher L values.

Concluding Remarks

On the basis of our analysis of the AP-8 flux distribution, it appears that the drift shell averaged density n_a is very effective in organising fluxes for the lowest L values, and may therefore be considered a good candidate to replace L as a coordinate for the low-altitude environment.

It should be kept in mind that the AP-8 models are extrapolated and smoothed averages of a number of data sets, so that it would be preferable to look at original data sets, old or new, which have a better resolution at low altitudes. To this effect, we have started to re-analyse the AZUR proton data. The AZUR satellite [*Hovestadt et al.*, 1972] operated from November 1969 to June 1970 in a polar orbit with perigee 383 km, apogee 3145 km and inclination 103°. It measured proton fluxes along two pitch angles, 90° and 45°, in six energy channels between 1.5 MeV and 104 MeV. The low-altitude part of AP-8 MAX is based on the AZUR proton data set.

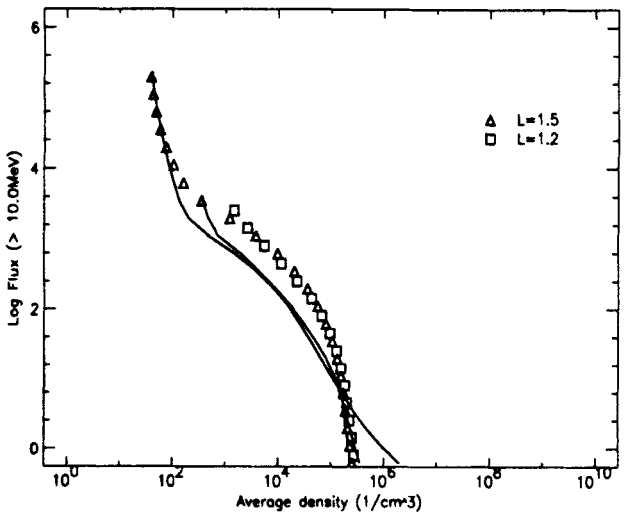

Fig. 4. The integral AP-8 MIN/MAX proton flux above 10 MeV as a function of the drift shell average of the atmospheric density for low L-values. The symbols and lines have the same meaning as in Fig. 1.

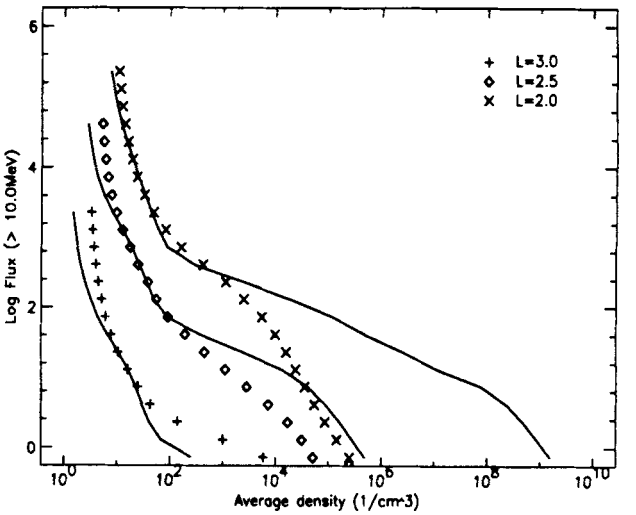

Fig. 5. The integral AP-8 MIN/MAX proton flux above 10 MeV as a function of the drift shell average of the atmospheric density for higher L-values. The symbols and lines have the same meaning as in Fig. 1.

Acknowledgments. We thank E.J. Daly and H. Evans for many stimulating and fruitful discussions. We thank C.E. McIlwain for providing a revised version of Hassitt's program. We also thank D. Bilitza and V. Pierrard for providing the MSIS and IRI codes and the cross section program CROSS. This work was funded by ESA contract No. 9828/92/NL/FM.

References

Bailey, D.K., Abnormal ionization in the lower ionosphere associated with cosmic-ray flux enhancements, *Proc. IRE*, **47**, 255–266, 1959.

Bilitza, D., International Reference Ionosphere 1990, National Space Science Data Center, NSSDC/WDC-A-R&S 90-20, 1990.

Carpenter, D.L., and Anderson, R.R., An ISEE/Whistler Model of Equatorial Electron Density in the Magnetosphere, *J. Geophys. Res.*, **97**, 1097–1108, 1992.

Daly, E.J., and Evans, H.D.R., Problems in Radiation Environment Models at Low Altitudes, Memorandum ESA/ESTEC WMA/93-067/ED, 1993.

Hassitt, A., An average atmosphere for particles trapped in the Earth's magnetic field, University of California at San Diego, 1964.

Hassitt, A., Average Effect of the Atmosphere on Trapped Protons, *J. Geophys. Res.*, **70**, 5385–5394, 1965.

Hedin, A.E., Extension of the MSIS thermosphere model into the middle and lower atmosphere, *J. Geophys. Res.*, **96**, 1159–1172, 1991.

Heynderickx, D., Pierrard, V., and Lemaire, J., Atmospheric Cut-Off, Technical Note 2 of the TREND-2 Study, ESTEC Contract No. 9828/92/NL/FM, 1994.

Hovestadt, D., Achtermann, E., Ebel, B., Haüsler, B., and Pachmann, G., New observations of the proton population of the radiation belt between 1.5 and 104 MeV, *Earth's Magnetospheric Processes*, B.M. McCormac (ed.), D. Reidel Publishing Company, Dordrecht, Holland, 115–119, 1972.

Kamiyama, H., Ionization and excitation by precipitating electrons, *Rep. Ionos. Space Res. Japan*, **20**, 171–187, 1966.

Lenchek, A.M., and Singer, S.F., Geomagnetically trapped protons from cosmic-ray albedo neutrons, *J. Geophys. Res.*, **67**, 1263–1287, 1962.

McIlwain, C.E., Coordinates for Mapping the Distribution of Magnetically Trapped Particles, *J. Geophys. Res.*, **66**, 3681–3691, 1961.

Newkirk, L.L., and Walt, M., Longitudinal drift velocity of geomagnetically trapped particles, *J. Geophys. Res.*, **69**, 1759–1763, 1964.

Pfitzer, K.A., Radiation Dose to Man and Hardware as a Function of Atmospheric Density in the 28.5 Degree Space Station Orbit, MDSSC Report No. H5387 Rev A, 1990.

Pierrard, V., Cross sections for collisions between electrons or protons and the main atmospheric components, *Aeronomica Acta*, **54**, 1994.

Ray, E.C., On the Theory of Protons Trapped in the Earth's Magnetic Field, *J. Geophys. Res.*, **65**, 1125–1134, 1960.

Rees, M.H., Auroral ionization and excitation by incident energetic electrons, *Planet. Space Sci.*, **11**, 1209–1218, 1963.

Sawyer, D.M., and Vette, J.I., AP-8 Trapped Proton Environment for Solar Maximum and Solar Minimum, NSSDC/WDC-A-R&S 76-06, 1976.

Vette, J.I., The AE-8 Trapped Electron Model Environment, NSSDC/WDC-A-R&S 91-24, 1991.

D. Heynderickx and J. Lemaire, Belgian Institute for Space Aeronomy, Ringlaan 3, B-1180 Brussels, Belgium. (e-mail addresses: dh@plasma.oma.be; jl@plasma.oma.be)